

Electronic Supplementary Information (ESI)

Graphene Oxide-Mediated Polyelectrolyte with High Ion-Conductivity for Highly Stretchable and Self-healing All-Solid-State Supercapacitors

Xuting Jin, Guoqiang Sun, Hongsheng Yang, Guofeng Zhang, Yukun Xiao, Jian Gao, Zhipan Zhang*, Liangti Qu*

Key Laboratory of Photoelectronic/Electrophotonic Conversion Materials, Key Laboratory of Cluster Science, Ministry of Education of China, School of Chemistry and Chemical Engineering, Beijing Institute of Technology, Beijing 100081, P. R. China.

*Email: zhipan@bit.edu.cn, lqu@bit.edu.cn

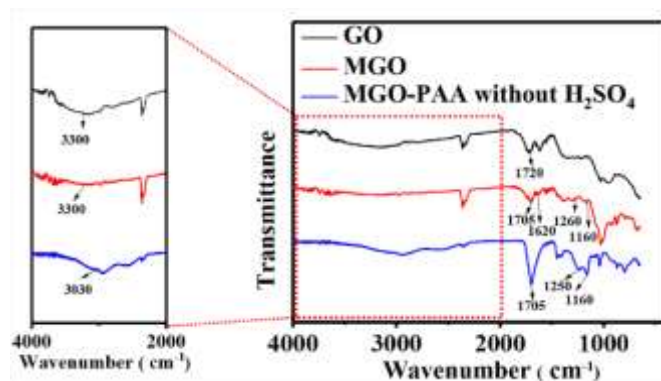


Fig. S1. Fourier transform infrared (FTIR) spectrum of GO, MGO and MGO-PAA without H_2SO_4 . The absorption band at 1620 cm^{-1} is attributed to the presence of vinyl groups in MGO [S1]. Existence of the (-Si-O-C) bond is confirmed by the absorption at 1160 cm^{-1} in MGO and MGO-PAA [S2]. The 1250 cm^{-1} in MGO-PAA and 1260 cm^{-1} in MGO represent the vibrant presence of the C-C(=O)-O group [S2]. The presence of a vibrant carbonyl (-C=O) group is confirmed proved by the band at 1720 cm^{-1} and 1705 cm^{-1} [S1]. The band O-H stretching vibrations are observed at 3300 cm^{-1} in GO and MGO, and at 3030 cm^{-1} in MGO-PAA. The polymerization between the vinyl groups of MGO and AA is easily occurred in the existence of ammonium persulfate (APS).

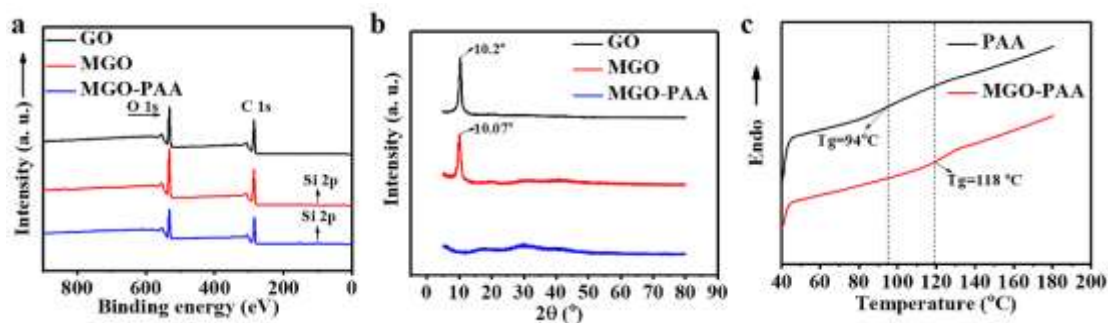


Fig. S2. a) X-ray photoelectron spectroscopy (XPS) results of GO, MGO and MGO-PAA with 0.33 wt% of MGO contents. For GO, no Si signals were observed in the range of 95-110 eV, but a weak Si 2p signal (101.98 eV) can be identified in MGO and MGO-PAA [S3]. These results can also confirm that MGO and MGO-PAA were prepared successfully. b) X-ray diffraction(XRD) patterns of dried GO, MGO and MGO-PAA with 0.33 wt% of MGO contents. First, the diffraction peaks at 10.2° and 10.07° were observed in GO and MGO, respectively. However, the MGO-PAA hydrogel was the absence of the diffraction peaks at 10.2° and 10.07°. Accordingly, the result may imply the uniform dispersion of GO nanosheets in the MGO-PAA hydrogel. c) The glass transition temperature (T_g) of dried PAA, MGO-PAA with 0.33 wt% of MGO contents. Apparently, MGO-PAA hydrogel (118 °C) exhibits higher T_g than neat PAA (94 °C), indicating the formation of cross-linking structure in the MGO-PAA hydrogel.

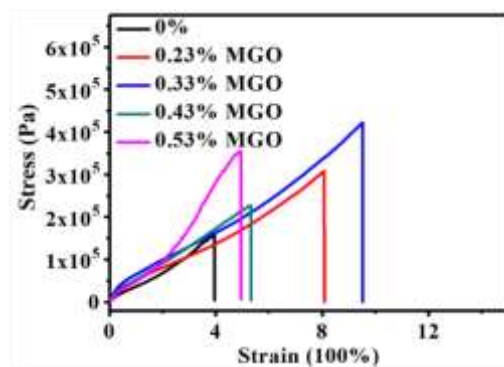


Fig. S3. Stress-strain curves of MGO-PAA polymer electrolytes (60 wt% water content) with various MGO content relative to AA monomers.

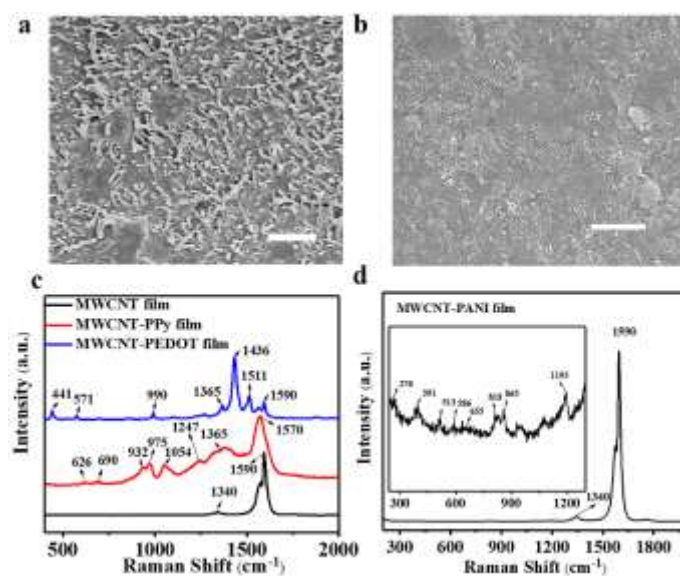


Fig. S4. a) The SEM image of MWCNT-PEDOT films. Scale bar, 5 μm. b) The SEM image of MWCNT-PANI films. Scale bar, 5 μm. c) Raman spectra of MWCNT, MWCNT-PPy and MWCNT-PEDOT films. d) Raman spectra of MWCNT-PANI film. The D band and the G band peaks of MWCNT films are observed at 1340 cm⁻¹ and 1590 cm⁻¹, respectively. In the Raman spectra of MWCNT-PPy films, the peaks ranged from 629 to 1247 cm⁻¹ can be ascribed to the characteristic peaks of PPy besides these two typical peaks of MWCNT films [S4]. The characteristic peaks of PEDOT can be obtained in the Raman spectra of MWCNT-PEDOT film. In Fig. S3d, those peaks ranged from 270 to 1195 cm⁻¹ can be attributed to the characteristic peaks of PANI.

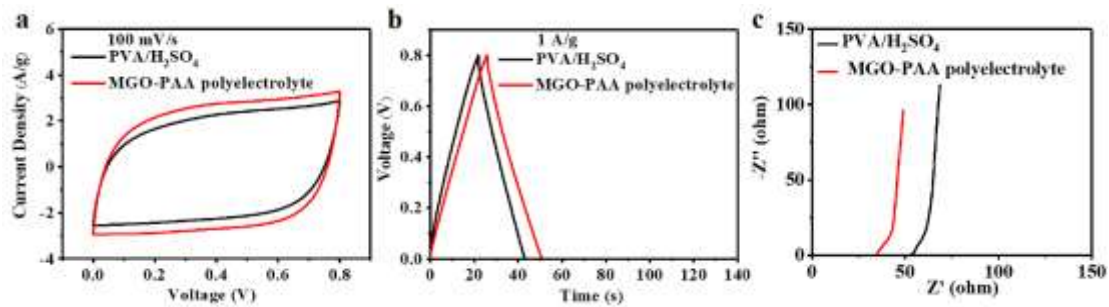


Fig. S5. The CV, GCD, and EIS curves of the supercapacitors assembled by the MGO-PAA polyelectrolyte with 70 wt% water content and PVA/H₂SO₄. The specific capacitance of the assembled SC with MGO-PAA polyelectrolyte is 62.7 F/g at the current density of 1 A/g. In comparison, the specific capacitance of SC with frequently-used PVA/H₂SO₄ as electrolyte is 54.7 F/g with the same MWCNT-PPy films as electrodes at the current density of 1 A/g. More importantly, the assembled SC with MGO-PAA polyelectrolyte possesses lower impedances than the SC with PVA/H₂SO₄ electrolyte. These results may be attributed to high ionic conductivity of MGO-PAA polyelectrolyte.

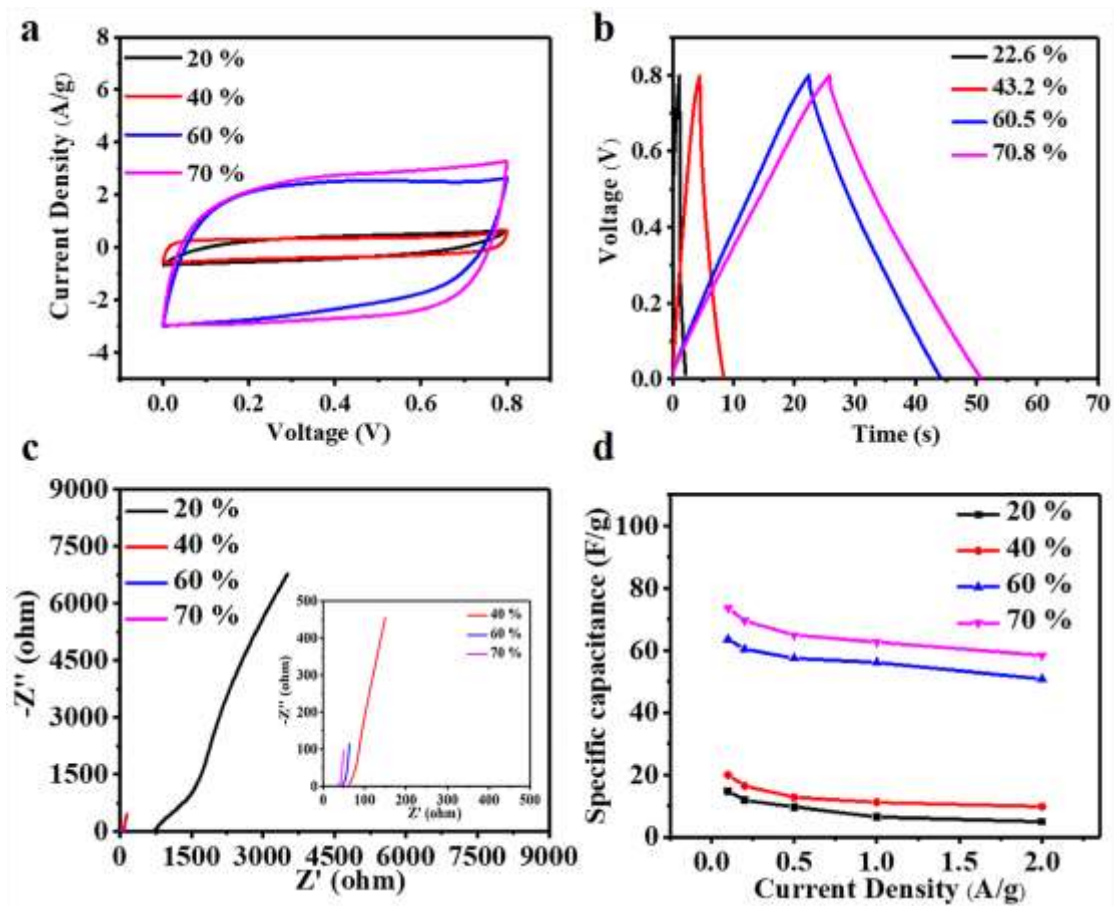


Fig. S6. a) The CV at 100 mV/s, b) GCD at 1 A/g, c) EIS curves and d) rate performance of the supercapacitor assembled by MWCNT-PPy films and MGO-PAA polymer electrolytes with various water content.

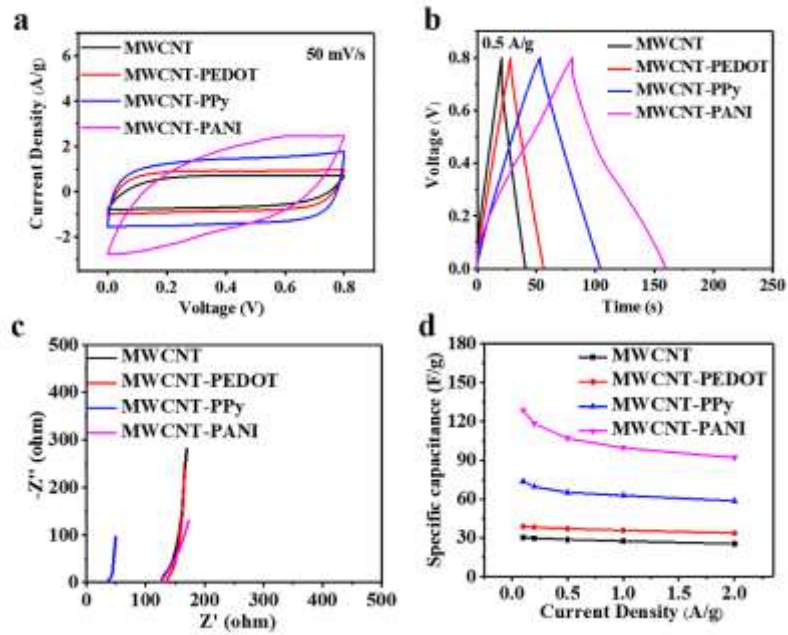


Fig. S7. a) The CV at 100 mV/s, b) GCD at 1A/g, c) EIS curves and d) rate performance of SCs assembled by various MWCNT-based electrodes and the MGO-PAA polymer electrolytes with 70 wt% water content. The SC with the MWCNT-PANI film showed the best specific capacitance of 128.6 F/g at the current density of 0.1 A/g in the absence of additional current collectors. Despite the absence of additional current collectors, the specific capacitances of MWCNT, MWCNT-PEDOT and MWCNT-PPy films also reach to 29.4 F/g, 38.1 F/g and 73.7 F/g at the current density of 0.1 A/g, respectively. Meanwhile, the assembled SCs based on MGO-PAA polyelectrolytes have the low impedance values as shown in Fig. S7. These results indicate that MGO-PAA hydrogel is an ideal candidate as polyelectrolyte for the SC application.

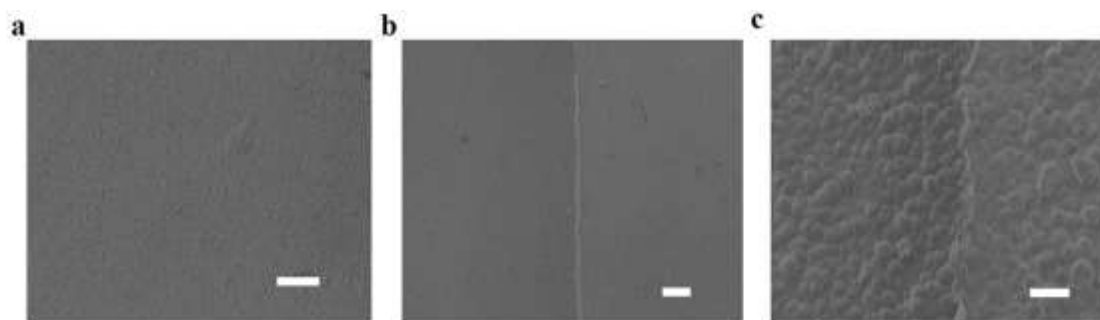


Fig. S8. a) SEM image of MWCNT-PPy films of the SC assembled by the MGO-PAA polyelectrolyte. Scale bar, 100 μm . b) SEM image and c) enlarged view of MWCNT-PPy films of the assembled SC after healing. Scale bar is 100 μm and 10 μm , respectively.

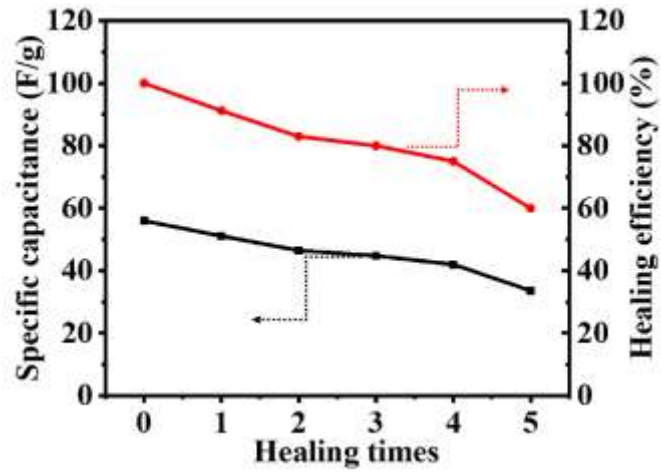


Fig. S9. The specific capacitances and healing efficiency calculated from the discharge curves as a function of healing time.

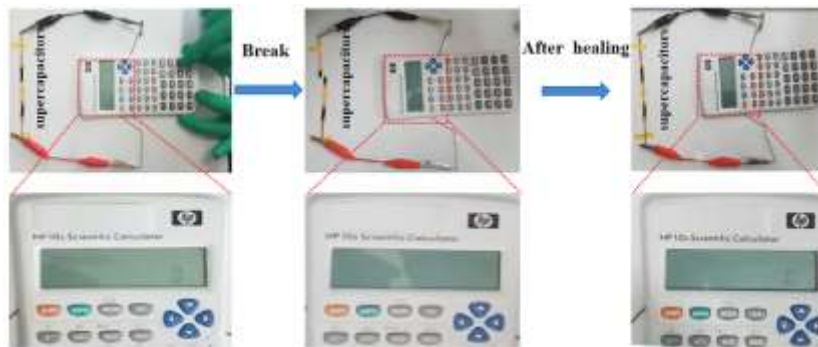


Fig. S10. The photographs of two SCs connected in series, one of which has been broken, powering a commercial calculator after self-healing without being recharged.

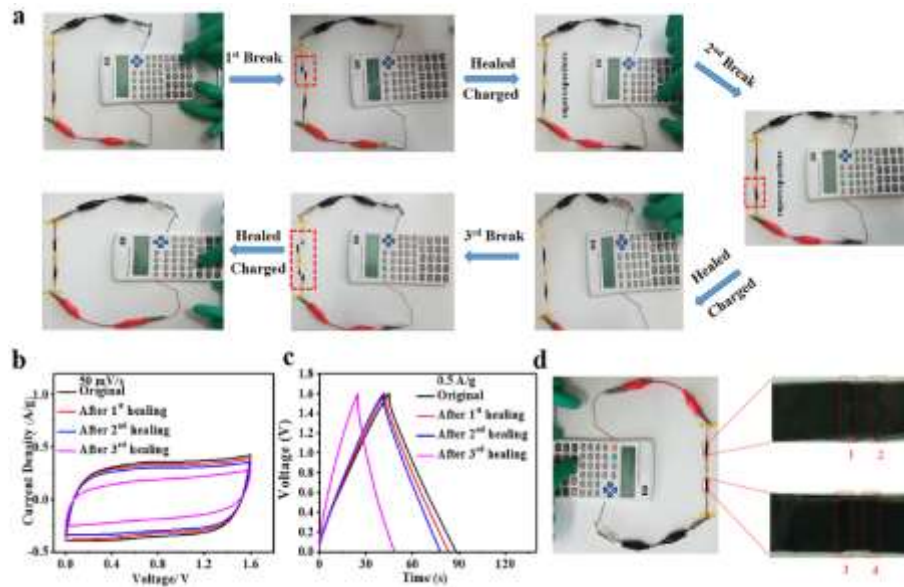


Fig. S11. a) The photographs of two SCs connected in series to power a commercial calculator after different cutting/healing cycles. b) The CV curves and c) GCD curves of two SCs connected in series after different cutting/healing cycles. d) The photograph of a commercial calculator powered by two SCs in series after 3rd self-healing.

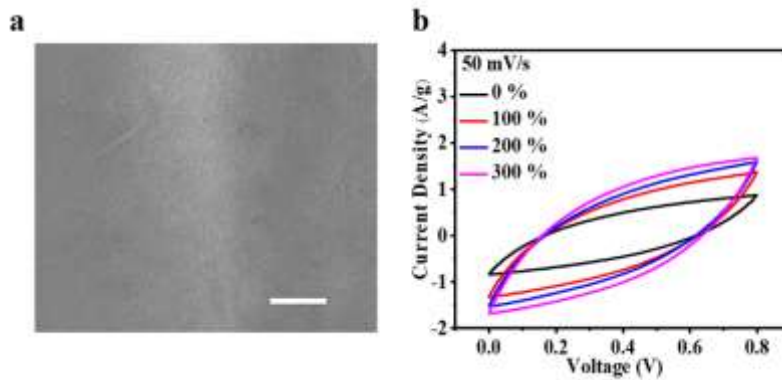


Fig. S12. a) SEM image of MWCNT-PPy films on the stretched SC. b) CV curves of various stretch ratios at the scan rate of 50 mV/s.

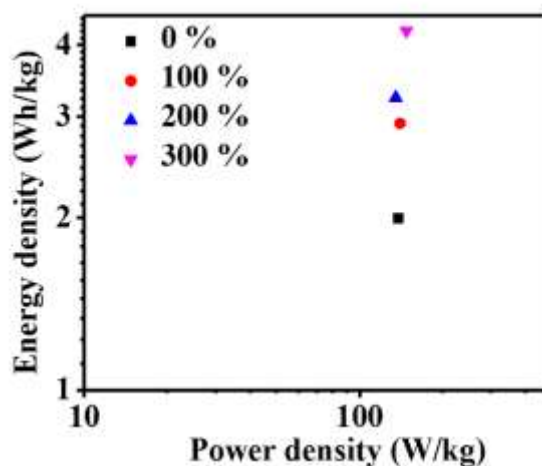


Fig. S13. Ragone plots of the stretchable SC under stretching ratios of 100%, 200% and 300%. The energy density E (Wh/kg) and the power density P (W/kg) were evaluated by means of GCD curves following the equations: $E=1000C_s (\Delta V)^2/7200$, $P=3600E/\Delta t$. The energy density of the stretchable SC increases from 2 to 4.23 Wh/kg when the device was stretched to 300 %.

Reference

- [S1] G. He , C. Chang , M. Xu , S. Hu , L. Li , J. Zhao , Z. Li , Z. Li , Y. Yin , M. Gang , H. Wu , X. Yang , M. D. Guiver, Z. Jiang, *Adv. Funct. Mater.* 25 (2015) 7502-7511.
- [S2] A. N. Mondal, C. Cheng, M. I. Khan, M. M. Hossain, K. Emmanuel, L. Ge, B. Wu, Y. He, J. Ran, X. Ge, N. U. Afsar, L. Wu, T. Xu, *J. Membr. Sci.* 525 (2017) 163-174.
- [S3] P. Wang, J. Zhang, L. Dong, C. Sun, X. Zhao, Y. Ruan, H. Lu, *Chem. Mater.* 29 (2017) 3412-3422.
- [S4] J. Wang, Y. L. Xu, F. Yan, J. B. Zhu, J. P. Wang, *J. Power Sources* 196 (2011) 2373-2379.